Oriented Crystalline Monolayers and Bilayers of 2 × 2 Silver(I) Grid Architectures at the Air–Solution Interface: Their Assembly and Crystal Structure Elucidation

Isabelle Weissbuch,*[a] Paul N. W. Baxter,[d] Ivan Kuzmenko,[a] Hagai Cohen,[a] Sidney Cohen,[a] Kristian Kjaer,[b] Paul B. Howes,[b] Jens Als-Nielsen,[c] Jean-Marie Lehn,*[d] Leslie Leiserowitz,*[a] and Meir Lahav*[a]

Abstract: Oriented crystalline monolayers, ~14 Å thick, of a 2 × 2 Ag^+ grid complex, self-assembled at the air–solution interface starting from an water-insoluble ligand 3,6-bis[2-(6-phenylpyridine)]pyridazine spread on silver-ion-containing solutions, were examined by grazing-incidence X-ray diffraction and specular X-ray reflectivity using synchrotron radiation. The monolayer structure was refined, including a determination of the positions of the counterions, with the SHELX-97 computer program. The monolayers were transferred from the interface onto various solid supports and visualized by scanning force microscopy, and characterized by X-ray photoelectron spectroscopy in terms of molecular structure. On surface compression, the initial self-assembled monolayer undergoes a transition to a crystalline bilayer in which the two layers, almost retaining the original arrangement, are in registry. Such a phase transition is of relevance to the understanding of crystal nucleation.

Keywords: N ligands · self-assembly · silver · structure elucidation · supramolecular chemistry · thin films

Introduction

In our earlier studies, reactions at the air–solution interface that involve both insoluble and soluble species have led to products of complex architecture that self-assemble as two-dimensional crystalline films of nanometer thickness.[1–7] Inorganic supramolecular systems in the form of racks, ladders, grids, and cages have previously been reported to self-assemble in bulk solution.[8–13] The coordination array in such systems could be assembled from either tridentate ligands and octahedral metal ions or from bidentate ligands and tetrahedral metal ions.

The approach of combining the reactivity of formation of supramolecular systems with the possibility of performing these reactions at interfaces has yielded 3 × 3 grids of nine Ag^+ ions coordinated to six ligand molecules (L), $[Ag_9L_6]^{9+}[(CF_3SO_3)_9]^{9-}$ that self-assemble into monolayer or bilayer crystalline films.[14] We provided evidence that the 3 × 3 Ag^+ grid complex cation, once formed, self-assembles with counterions (that make the salt insoluble in water) into oriented crystalline domains of structure akin to that of the corresponding macroscopic crystal. A lateral aggregation process is favored at interfaces, and the resulting structure contains a small number of layers. Such films, being of potential interest for microelectronic technology, were transferred onto solid surfaces.

Here, we apply the above-mentioned approach to the self-assembly of crystalline monolayers, ~14 Å thick, of a 2 × 2 grid complex $[Ag_4L_4]^{4+}[(CF_3SO_3)_4]^{4-}$ (**2**), which contains four Ag^+ ions coordinated to four 3,6-bis[2-(6-phenylpyridine)]-pyridazine ligands (**1**),[12] oriented at the air–solution interface. The crystalline films were examined by grazing-incidence X-ray diffraction (GIXD) and specular X-ray reflectivity (XR) with synchrotron radiation at the air–solution interface. The monolayer structure was refined, including a determination of the positions of the counterions, by

[a] Dr. I. Weissbuch, I. Kuzmenko, Dr. H. Cohen, Dr. S. Cohen, Prof. Dr. L. Leiserowitz, Prof. Dr. M. Lahav
Department of Materials and Interfaces
The Weizmann Institute of Science, 76100 Rehovot (Israel)
Fax: (+972) 8-934-4138
E-mail: csweisbu@weizmann.ac.il

[b] Dr. K. Kjaer, Dr. P. B. Howes
Condensed Matter Physics and Chemistry Department
Risø National Laboratory, 4000 Roskilde (Denmark)

[c] Prof. Dr. J. Als-Nielsen
Niels Bohr Institute
H. C. Ørsted Laboratory, 2100 Copenhagen (Denmark)

[d] Prof. Dr. J.-M. Lehn, Dr. P. N. W. Baxter
Laboratoire de Chimie Supramoléculaire
Institut Le Bel, Université Louis Pasteur
67000 Strasbourg (France)

  0947-6539/00/0604-0725 $ 17.50+.50/0

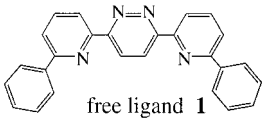

free ligand **1**

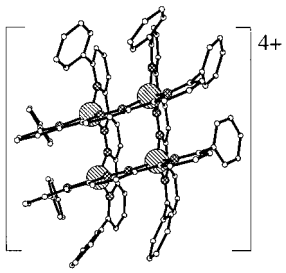

2x2 Ag^{+} grid complex **2**

using the SHELX-97 computer program. The films were transferred from the interface onto various solid supports and characterized by scanning force microscopy (SFM) and by X-ray photoelectron spectroscopy (XPS) in terms of molecular structure. This system represents the first reported case in which, through surface compression of the initial self-assembled crystalline monolayer, the film undergoes a transition to a crystalline bilayer in which the two layers, almost retaining the original arrangement, are in registry. Such a phase transition is of relevance to the understanding of crystal nucleation.

Results and Discussion

The first indication of the reaction that involved the free ligand molecules **1** spread on an aqueous subphase which contained silver triflate (CF_3SO_3Ag, 1 mM) was obtained from the surface pressure area (Π-A) isotherms (Figure 1). The isotherm of the free ligand molecules spread on pure water displays a plateau in the range of nominal mean molecular areas of ~40 to 10 Å^2, followed by a steep increase in surface pressure. In contrast, the isotherm of the same molecules spread on a 1 mM silver triflate solution shows a slow increase in surface pressure only at a nominal mean molecular area lower than ~25 Å^2 and a small plateau in the range of ~9.5 to 5 Å^2. The isotherm measured on a 1 mM (1:1) silver triflate/silver acetate solution shows even a smaller increase in pressure at the plateau between ~25 to 12 Å^2 (Figure 1). The

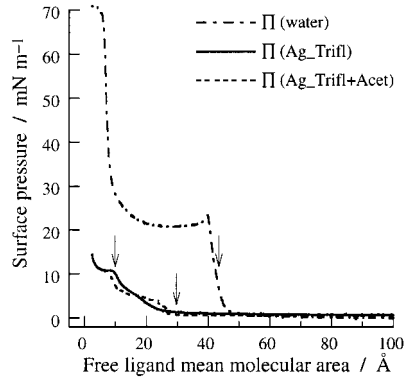

Figure 1. Surface pressure area isotherms of ligand **1** spread on pure water, on a 1 mM CF_3SO_3Ag aqueous solution and on a 1 mM (1:1) CF_3SO_3Ag/CH_3CO_2Ag aqueous solution. Arrows indicate the points along the isotherms at which GIXD and XR measurements were performed.

isotherm measured on a 1 mM silver acetate (CH_3CO_2Ag) solution shows no increase in surface pressure over the whole area range. These results are indicative of an interfacial reaction followed by film formation of a product that is less soluble in silver triflate solution than in the other two subphases.

Independent information on the morphology of the film was obtained from the scanning force microscopy (SFM) images measured after film transfer from the liquid surface onto a freshly cleaved mica support (Figure 2). The SFM topography images obtained from the free ligand spread on pure water show isolated, thick, elongated crystallites (Figure 2a). The images taken from the free ligand spread onto the silver triflate solution are completely different (Figure 2b); they show rounded domains, ~12 Å thick, that, presumably, were transferred onto the silver triflate film, of

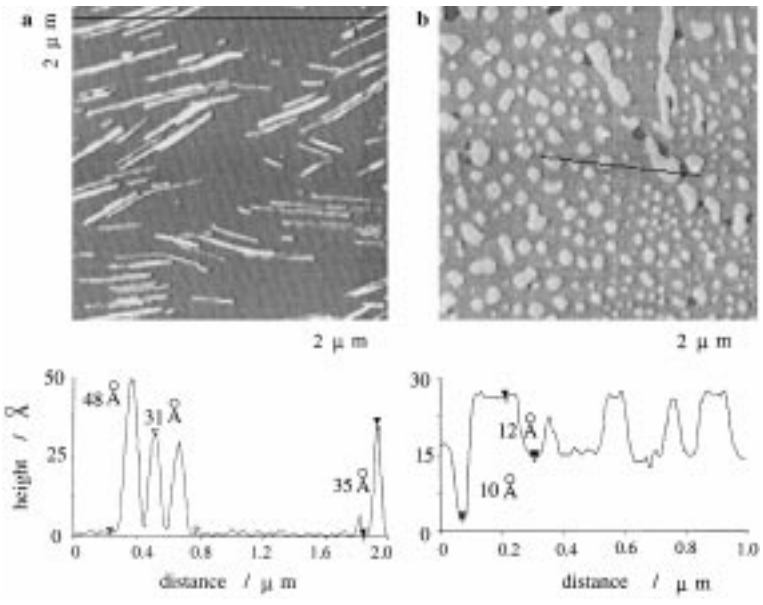

Figure 2. SFM topography images and height analyses of samples prepared by spreading the same amount of free ligand **1** molecules on a) pure water and b) 1 mM CF_3SO_3Ag aqueous solution, and subsequent transfer from the liquid surface onto a mica support. The height analyses are along the "black lines" of the images. Note that in b) 10 Å is the depth of the "hole" in the silver triflate that absorbed on the mica prior to the deposition of the grid film.

0947-6539/00/0604-0726 $ 17.50+.50/0 *Chem. Eur. J.* **2000**, *6*, No. 4

thickness ~5–10 Å, which had already adsorbed onto the mica. Occasionally, domains of greater thickness (~25 Å) were also observed.

Evidence for the molecular structure of complex **2**, self-assembled at the air–solution interface, was obtained from X-ray photoelectron spectroscopy measurements (XPS). Film samples, transferred onto glass supports, were compared with two reference samples: the free ligand and a 2×2 Ag^+ grid complex prepared in nitromethane solution.

As previously reported,[14] the N(1s) line of the free ligand molecule **1** consists of two components with an intensity ratio of 1:1 and a binding energy split of 0.8 eV, attributed to the N atoms of the pyridine ($2N_1$ atoms) and pyridazine ($2N_2$ atoms) rings (Figure 3a).

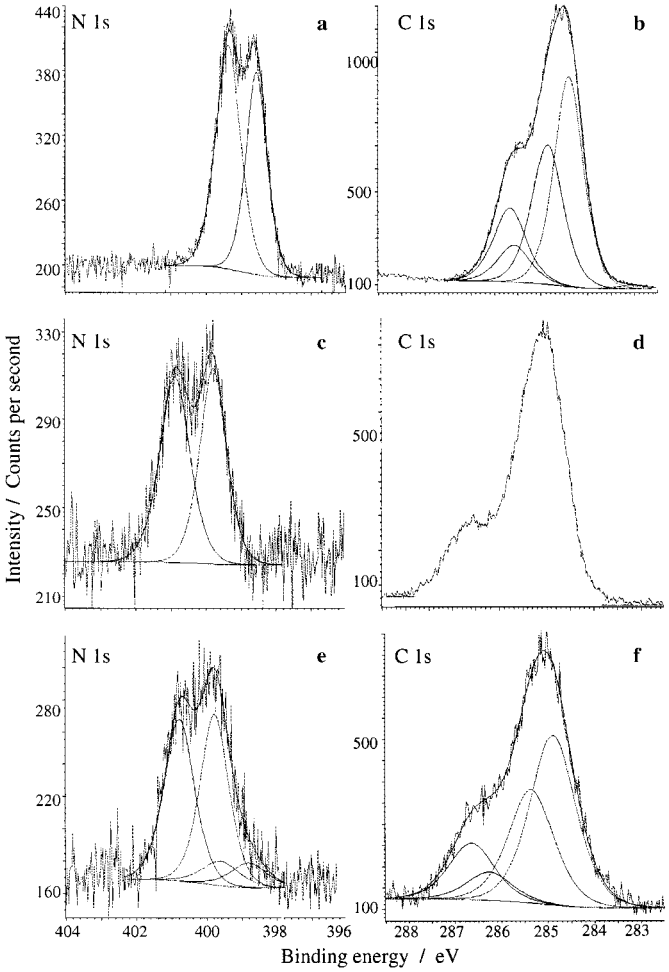

Figure 3. XPS data shown for the N(1s) and C(1s) lines of free ligand **1** (a,b), the 2×2 Ag^+ grid **2** prepared in bulk solution (c,d), and films of **2** self-assembled at the air–solution interface (e,f) and transferred onto a glass support.

In the 2×2 Ag^+ grid complex prepared in bulk solution, pronounced shifts of 1.2 eV and 1.5 eV were observed for the N_1 and N_2 lines (Figure 3c); this reflects the coordination between the N atoms and the Ag^+ ions in the grid complex. The same shifts were obtained for the N atoms lines in the grid films self-assembled at the air–solution interface, (Figure 3e), indicative of a basically similar structure to the grid complex prepared in the bulk solution (Table 1). The N(1s) data of the grid film (Figure 3e) could be best fitted by assuming an additional pair of lines (with intensity ratio 1:1), which represent 15% of the total N mass, at 0.2 eV higher binding energies than the corresponding lines of the free ligand. Several repeat measurements on the same spot showed that these lines increased, after 4.5 hours, to 84% of the total N mass, indicative of beam damage.

Table 1. Curve fitting results for the N 1s and C 1s photoelectron lines (number of atoms given in parentheses). Peak positions are given in eV and are calibrated with respect to the Si(2p) line (103.3 eV).

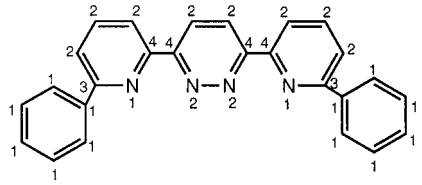

	N 1s		C 1s			
	N_1 (2)	N_2 (2)	C_1 (12)	C_2 (8)	C_3 (2)	C_4 (4)
free ligand **1**	398.6	399.4	284.4	284.9	285.6	285.7
grid **2** bulk	399.8	400.9	285.0	285.4	286.3	286.8
grid **2** film	399.8	400.8	284.9	285.4	286.3	286.7
	398.8	399.6				
$\Delta_{(grid-ligand)}$	1.2	1.5	0.5	0.5	0.7	1.0

Binding energy shifts consistent with the formation of the grid have also been observed for the C(1s) lines (Table 1). The C(1s) line of the free ligand, spread on water and transferred onto a glass support, was analyzed in terms of four types of C atoms, C_1 (12 C atoms), C_2 (8 C atoms), C_3 (2 C atoms), and C_4 (4 C atoms), (see labels in Table 1). This consideration leads to four components for the C(1s) line, which was fitted by constraining their intensity ratio (Figure 3b and Table 1). The same curve-fitting procedure[15] was applied to the C(1s) line of the grid film, prepared from the same amount of free ligand spread on a silver triflate solution, (Figure 3d), leading to a pronounced site selective shift in binding energy. The largest shift was observed for the C atoms adjacent to the N atoms (Table 1), namely, C_3 and C_4 were shifted by 0.7 eV and 1.0 eV, respectively, whereas C_1 and C_2 were both shifted by 0.5 eV. The pronounced binding energy shifts of both the N(1s) and the C(1s) lines represent fingerprint evidence for the 2×2 Ag^+ complex formation.

Independent structural information on the self-assembled film of 2×2 Ag^+ grids was obtained from specular X-ray reflectivity (XR) measurements performed in situ at the air–solution interface. The X-ray reflectivity curve, R/R_F, measured from the self-assembled film and normalized to the Fresnel reflectivity of a perfectly reflecting surface is shown in Figure 4. The calculated curve was obtained by using a three-box model (Table 2) with the constraint of the structure of the complex **2** and the orientation determined from the grazing-incidence X-ray diffraction (GIXD) results described in the following section. From these results, two models of the electron density distribution along the direction perpendicular to the liquid surface were feasible: one model assumes that complex **2** is oriented with the plane of the Ag^+ ions perpendicular to the surface, and the second model assumes a parallel orientation. The electron density of each box was

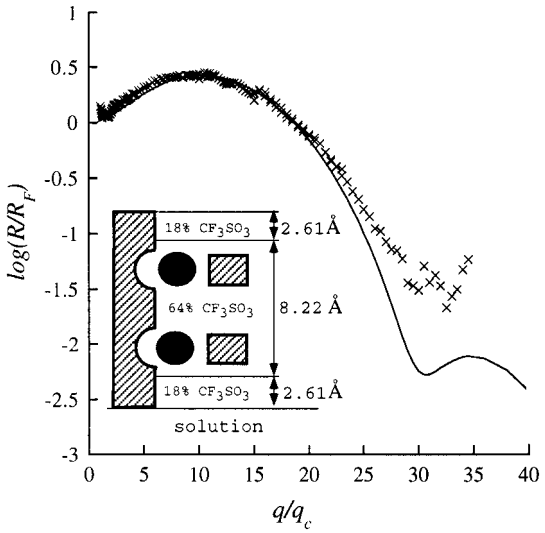

Figure 4. Measured (points) and calculated (solid line) X-ray reflectivity curves, expressed as normalized R/R_F for ligand **1** spread on 1 mM CF_3SO_3Ag aqueous solution. Inset: Schematic representation of the 2×2 Ag^+ grid orientation showing the length, in the direction normal to the surface, of the three-box model together with the proposed distribution of the counterions. The shaded patterns represent a side view of the four ligands and the two black circles the side view of the 2×2 Ag^+ grid cation.

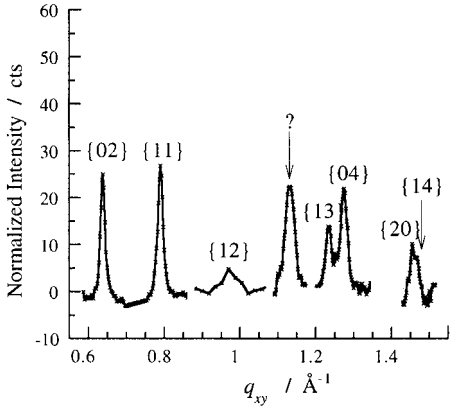

Figure 5. Measured GIXD pattern of ligand **1** spread on water for a nominal mean molecular area of 40 Å^2, presented as intensity distribution $I(q_{xy})$ and showing the Bragg peaks. The ? sign indicates the reflection with no assigned Miller index.

calculated from the number of electrons of the constituent atoms, the length determined from the geometry of complex **2**, and the area occupied by the complex estimated from the GIXD results. To these values, the electron density corresponding to the number of triflate counterions for charge neutrality was added and distributed within each box to yield a better fit to the measured reflectivity curve.

The best fit to the measured reflectivity curve (Figure 4) was obtained when complex **2** was oriented with the plane of the Ag^+ ions perpendicular to the surface, and a distribution of 18%, 64%, and 18% from the total number of electrons of the triflate counterions in the three boxes, as shown schematically in the inset of Figure 4. The fit parameters are listed in Table 2. The model involving the alternative orientation of the grid complex did not yield a dip at $q/q_c = 30$ in the reflectivity curve, an experimentally observed feature that has been reproduced several times.[16]

The results of the XR measurements are certainly in keeping with a film composed of a 2×2 Ag^+ grid complex with the plane of the Ag^+ ions oriented perpendicular to the solution surface.

Analysis of the grazing-incidence X-ray diffraction data (GIXD)

*Free ligand **1** on water*: The GIXD pattern shown in Figure 5 was measured for the free ligand **1** spread on pure water for a nominal mean molecular area of 40 Å^2, which corresponds to the beginning of the Π-A isotherm plateau (Figure 1). The pattern contains eight Bragg peaks that could not be assigned according to a crystalline phase assuming a single orientation at the air–water interface. To illustrate this point, Table 3 shows the best attempt. A rectangular unit cell of dimensions $a = 8.7$ Å, $b = 19.6$ Å, $A_{cell} = 170$ Å^2, reproduces the positions of five (assigned {02}, {11}, {12}, {04} and {14}) of the eight reflections, gives small but significant deviations for the {13} and {20} peaks, and leaves the reflection at $q_{xy} = 1.13$ Å^{-1} unassigned, (d spacing 5.5 Å). The latter peak, we propose, may arise from a different orientation of the same crystallites.[17] Some of the Bragg rod intensity profiles exhibit modulations indicative of multilayer crystallites; this is in agreement with shape of the Π-A isotherm and the SFM images.

Table 3. Analysis of the GIXD data measured from the free ligand molecules **1** spread on pure water for a mean molecular area of ~40 Å^2. The calculated q_{xy} values are from the unit cell of dimensions $a = 8.7$ Å, $b = 19.6$ Å, $A_{cell} = 170$ Å^2.

Peak no.	q_{xy} [Å^{-1}] measured	{h,k} Miller index assigned	q_{xy} [Å^{-1}] calculated
1	0.64	{02}	0.64
2	0.79	{11}	0.79
3	0.97	{12}	0.97
4	1.13	not assigned	–
5	1.234	{13}	1.201
6	1.275	{04}	1.280
7	1.455	{20}	1.445
8	1.467	{14}	1.472

Table 2. Fitted parameters[a] for the three-box model of electron density corresponding to the X-ray reflectivity curve in Figure 4.

	Boxes	Cov. [%]	A [Å^2]	ρ_1/ρ_s	L_1 [Å]	ρ_2/ρ_s	L_2 [Å]	ρ_3/ρ	L_3 [Å]	L_T [Å]	σ [Å]
1 / CF_3SO_3Ag	3	65	207.5	0.963	2.61	1.638	8.22	0.963	2.61	13.44	3.5

[a] Cov. is the surface coverage of the grid complex estimated from the number of free ligand molecules and the area onto which they were spread; A is the area occupied by a 2×2 Ag^+ grid complex (25% of unit cell area from GIXD); ρ_s is the electron density of the subphase, 0.334 e Å^{-3}; ρ_1 (N_1 is the number of electrons = 174), ρ_2 ($N_2 = 934$), and ρ_3 ($N_3 = 174$) are the model electron densities of the first, second, and third boxes, respectively, where $\rho_i = N_i/AL_i$, and L_1, L_2, and L_3 are the length of the boxes, respectively; the total length $L_T = L_1 + L_2 + L_3$; σ represents the surface roughness parameter.

0947-6539/00/0604-0728 $ 17.50+.50/0 *Chem. Eur. J.* **2000**, *6*, No. 4

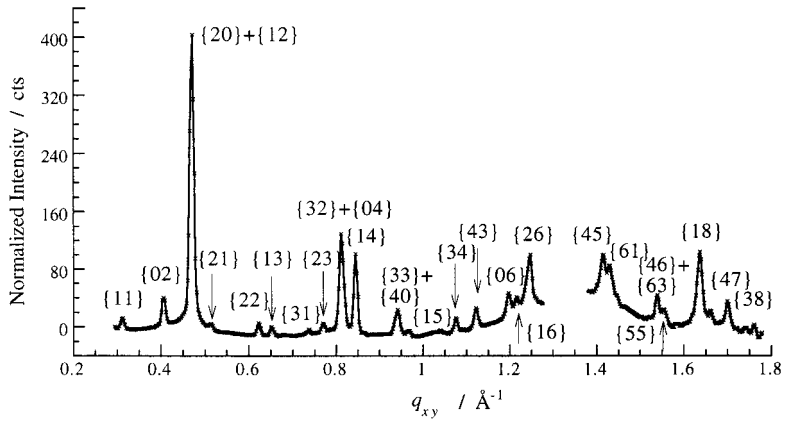

Figure 6. Measured GIXD data of ligand **1**, spread on a 1 mM CF_3SO_3Ag aqueous solution for a nominal mean molecular area of 30 Å^2, presented as intensity distribution $I(q_{xy})$, and showing the Bragg peaks with assigned (h,k) Miller indices.

*Free ligand **1** on CF_3SO_3Ag solution*

a) Self-assembled crystalline monolayer of a 2×2 Ag^+ grid complex: The GIXD pattern measured for the free ligand molecules **1**, spread for a nominal mean molecular area of $\sim$30 Å^2 on a 1 mM aqueous solution of silver triflate (Figure 6), is significantly different from that measured on pure water (Figure 5). $\{h,k\}$ Miller indices could be assigned to all 25 Bragg reflections[18] of the GIXD pattern, shown as an $I(q_{xy})$ scan in Figure 6, yielding a two-dimensional rectangular unit cell of dimensions $a=26.82$ Å, $b=30.95$ Å, $A_{cell}=830$ Å^2, (Table 4). As described above, the GIXD pattern of **1** spread on water could not be explained in terms of a single crystalline phase. In contrast, the pattern measured on the silver triflate solution is indicative not only of a single crystalline phase of an oriented film, but is also consistent with the self-assembly of the 2×2 Ag^+ grid complex **2** from **1** and the Ag^+ ions present in the subphase. Such a complex is easily formed in nitromethane solutions, but no ordered films could be obtained from re-dissolved crystalline powders spread on a water surface. Therefore, in situ complexation and two-dimensional crystallization at the air–solution interface appear to be the only way to produce single-phase crystalline films that are highly oriented with respect to the surface. Note that the Bragg rod intensity profiles, shown as a two-dimensional intensity contour plot $I(q_{xy},q_z)$ in Figure 7a for part of the GIXD pattern, have their intensity maxima peaking at $q_z=0$ Å^{-1},

Table 4. Analysis of the GIXD data measured from the crystalline monolayer of the 2×2 Ag^+ grid complex, $[Ag_4\mathbf{1}_4][(CF_3SO_3)_4]$ prepared at the air–solution interface. The calculated q_{xy} values are from the unit cell of dimensions $a=26.82$ Å, $b=30.95$ Å, $A_{cell}=830$ Å^2.

Peak no.	q_{xy} [Å^{-1}] measured	$\{h,k\}$ Miller index assigned	q_{xy} [Å^{-1}] calculated
1	0.310	{11}	0.310
2	0.406	{02}	0.406
3	0.470	{20}+{12}	0.468+0.469
4	0.512	{21}	0.511
5	0.621	{22}	0.620
6	0.650	{13}	0.653
7	0.731	{31}	0.731
8	0.769	{23}	0.768
9	0.810	{32}+{04}	0.812+0.812
10	0.843	{14}	0.845
11	0.940	{33}+{40}+{24}	0.930+0.937+0.938
12	1.040	{15}	1.041
13	1.074	{34}	1.074
14	1.122	{43}	1.118
15	1.197	{06}	1.218
16	1.245	{16}	1.240
17	1.250	{26}	1.305
18	1.390	{45}	1.381
19	1.415	{61}	1.420
20	1.430	{54}	1.425
21	1.540	{63}+{46}	1.532+1.537
22	1.550	{55}	1.550
23	1.638	{18}	1.641
24	1.700	{47}	1.702
25	1.760	{38}	1.770

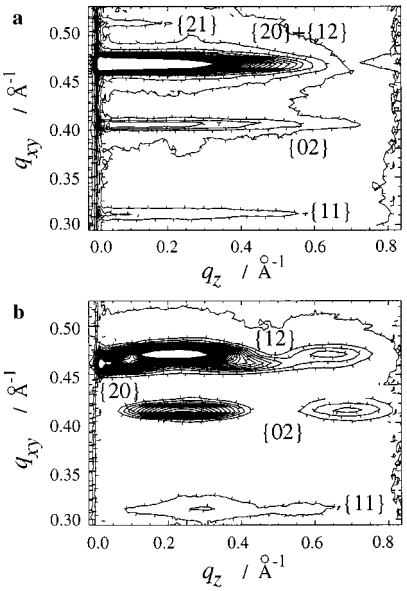

Figure 7. Measured GIXD patterns of ligand **1**, spread on a 1 mM CF_3SO_3Ag aqueous solution, presented as two-dimensional intensity contour plots $I(q_{xy},q_z)$ in the range $q_{xy}=0.3-0.55$ Å^{-1}. A comparison between the Bragg rod intensity distributions $I(q_z)$ in a) the self-assembled monolayer state and b) the compressed bilayer state of the film is also shown.

where q_z is the vertical component of the scattering vector. Their calculated full width at half maximum (FWHM) yielded an estimate of the total thickness of the film of $\sim$14 Å, indicative of a monolayer and in agreement with the results obtained from the XR and SFM measurements.

The calculated unit cell can be occupied by either two grid units oriented with the plane of the Ag^+ ions parallel to the surface or by four units oriented with the plane of the Ag^+ ions perpendicular to the surface, in terms of a molecular model.[19] The GIXD pattern (Figure 6) does not display $\{h,0\}$ reflections with $h=2n+1$ or $\{0,k\}$ with $k=2n+1$; this

indicates the plane group *pgg*. According to this plane group, which incorporates two perpendicular glide planes, the unit cell may contain either four symmetry related grid units in general positions or two grid units oriented with their twofold axes coinciding with the crystallographic twofold axes. The latter model was discarded on the basis of X-ray structure factor calculations. Thus the unit cell must contain four grid units oriented with their Ag^+ plane perpendicular to the liquid surface.

The lateral packing of the monolayer was determined, in the first approximation, by constructing a two-dimensional crystal in the plane group *pgg* and by finding the most probable position of the grid cation without counterions. This was done by comparing the $I\{h,k,0\}$ powder pattern calculated by means of the CERIUS[2] computer package with the measured q_z-integrated $I(h,k)$ pattern. The model structure was further improved by X-ray structure factor calculations from the SHELX-97 program.[20] In order to use this computer program (which is designed for three-dimensional crystal structures) to refine a two-dimensional powder (oriented with respect to the liquid surface but randomly oriented around the normal to the surface), the following procedure was adopted: i) in a two-dimensional crystal there is no intermolecular structural repeat along the direction normal to the *ab* plane, therefore the Bragg rod intensities $I\{h,k,q_z\}$ were assigned l Miller indices according to a long virtual c axis perpendicular to the *ab* plane; ii) the superposition of the Bragg rod intensities $I\{h,k,q_z\}$ and $I\{-h,-k,q_z\}$, obtained in the GIXD measurements, was simulated by assuming a twinning of the two-dimensional crystal about the *ab* plane.

In the first stage, the best model obtained by using CERIUS[2] was further refined in SHELX-97 in "space group" *Pba*2 by treating the grid unit as a rigid body with two translation and three rotation parameters. In the second stage, 27 triflate counterions per grid cation were placed in random positions that were refined together with their individual occupancies, but constrained to have a sum value of four, that is, equal to the number of counterions required per grid cation. By this procedure we discarded the counterions whose occupancies refined to zero or negative values, leading to a neutral structure with four counterions per grid unit, each of occupancy 1 ± 0.2. Finally, several more least-squares cycles were performed by alternate refinement of either the grid cation or the counterions. The best structure obtained has an agreement factor R_1 ($=\Sigma||F_s|-|F_c||/\Sigma|F_o|$, in which F_o and F_c are the observed and calculated structure factors) of 0.32 for the 660 observed intensities along the first eleven Bragg rods $I(h,k,q_z)$ of the GIXD pattern.[21] The structure was not further refined using all the reflections because of the uncertainty in the precise conformation of the grid cation, possible disorder of the counterions, and presence of water of solvation.

A comparison between the measured and calculated intensities along all of the eleven $\{h,k,q_z\}$ Bragg rods is shown in Figure 8, and the corresponding packing arrangement for the best obtained model is given in Figure 9. Note that the structure is the result of an attempt to apply the SHELX-97 computer program to refine a very complex two-dimensional crystal, and whose three-dimensional counterpart is unknown.

b) Crystalline multilayer: The GIXD pattern measured for the film, after its compression to one third of its initial occupied area, is shown in Figure 10 as an $I(q_{xy})$ scan and displays 15 Bragg reflections. All the reflections could be assigned $\{h,k\}$ Miller indices consistent with a single two-dimensional rectangular unit cell of dimensions $a = 26.86$ Å, $b = 30.43$ Å, $A_{cell} = 817$ Å^2, (Table 5). This unit cell is close in dimension to that of the crystalline monolayer phase that had been formed by self-assembly, indicating a similar in-plane layer structure.

The Bragg rod intensity profiles $I(q_z)$ are very different from those of the crystalline monolayer phase (Figure 7) despite the similarity in their unit cell dimensions. The two-dimensional intensity contour plot $I(q_{xy},q_z)$ of the monolayer phase (Figure 7a) shows that the first four Bragg reflections display intensity maxima at $q_z = 0$ Å^{-1}. In contrast, the contour plot for the same region of the pattern measured after film compression (Figure 7b) shows that the {11} and {02} Bragg peaks exhibit distinct intensity modulations with intensity maxima at $q_z > 0$ Å^{-1}. Moreover, the {20} + {12} Bragg peak of the monolayer phase at $q_{xy} = 0.470$ Å^{-1}, is now clearly separated into two Bragg rod intensity profiles: one, assigned as {20}, with intensity maxima at $q_z = 0$ Å^{-1} and 0.40 Å^{-1}, and the second, assigned as {12}, with intensity maxima at $q_z = 0.24$ Å^{-1} and 0.69 Å^{-1}. Similar intensity modulations were also observed for the other reflections of the compressed film.

The significant changes in the $I(q_z)$ profiles observed in the GIXD pattern upon compression of the film can be interpreted in terms of a phase transition from a crystalline monolayer to a crystalline multilayer, which, in all likelihood, retains the initial in-plane two-dimensional structure, in view of their unit cell dimensions.

We now address the structure of the multilayer film and how it was created. We may "attempt" a determination of the multilayer structure by assigning l Miller indices to the intensity modulations of the in-plane $\{h,k\}$ Bragg reflections, (Figure 11), in the following way: the *ab* plane of the multilayer is parallel to the liquid surface, and, therefore, the reciprocal unit vector c^* is normal to it. We assigned l indices 1 and 2 to the two intensity modulations of the $\{02q_z\}$ Bragg rod, (Figure 11). Hence, the Δq_z separation of 0.45 Å^{-1} between the two intensity modulations, which corresponds to a difference of one reciprocal unit vector along c^*, yields a d spacing of 14 Å ($1/c^* = 2\pi/0.45$ Å^{-1}) in the direction normal to the liquid surface. Moreover, we can derive that the {020} Bragg rod modulation should be at a q_z value of -0.2 Å^{-1}; this means that the reciprocal vector b^* is not in the *ab* plane, but has an out-of-plane component at a q_z value of -0.1 Å^{-1}. The reciprocal vector b^* has an in-plane component, b^*_{xy}, of length $1/b = 0.0329$ Å^{-1}, and an out-of-plane component, b^*_z, of length $0.1/2\pi = 0.0159$ Å^{-1}.

We fixed the direction of the reciprocal vector a^* by making use of the $\{20q_z\}$ Bragg rod for which l indices of 0 and 1 are assigned to the intensity maxima at $q_z = 0$ Å^{-1} and ~ 0.4 Å^{-1}; this means that a^* is in the *ab* plane and indeed parallel to a. The Δq_z separation of 0.4 Å^{-1} along the $\{20q_z\}$ Bragg rod is almost the same as that along the $\{02q_z\}$ Bragg rod. Based on these arguments, we attach l indices to the intensity modulations of all the Bragg rods to yield a reasonable match

0947-6539/00/0604-0730 $ 17.50+.50/0 *Chem. Eur. J.* **2000**, *6*, No. 4

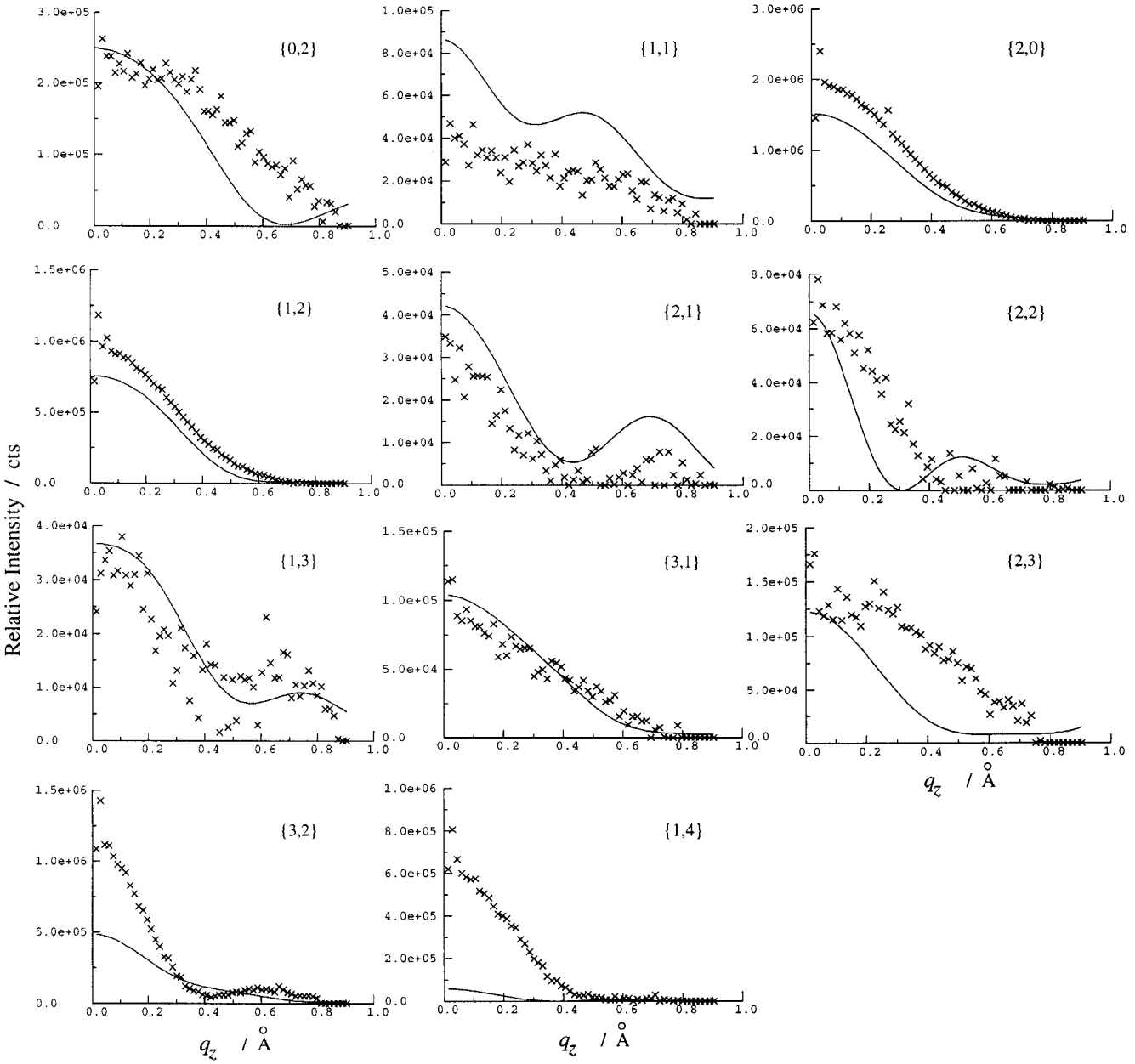

Figure 8. Comparison between the intensity profiles along q_z of the eleven (h,k,q_z) Bragg reflections from the self-assembled crystalline monolayer, as measured (points) and calculated (solid line) by SHELX-97 for the best model structure.

(Figure 11) and thus provide a measure of confidence in the l indices attached to the maxima of the $\{h,k,q_z\}$ Bragg rods.

Having determined the directions and magnitudes of a^*, b^*, and c^*, we derived the angle between c^* and the real space c axis as being 25.8°, that is, $\arctan(b_z^*/b_{xy}^*)$, and therefore the offset between neighboring layers as being equal to 6.7 Å [14/tan(25.8°)]. X-ray structure factor calculations, with an atomic coordinate model that contains two layers translated by 14 Å along the normal to the surface and offset by 6.7 Å along the b direction, yielded the Bragg rod intensity profiles shown in Figure 12 for three strong reflections. One can see that, although part of the calculated intensity follows the measured modulations, the intensity profiles could not be fitted. Other reflections, such as {22}, {04}, and {14} yielded a worse fit (not shown). From these calculations we can deduce that our proposed in-plane model structure of each of the layers is not quite correct. One may envisage that, during the film compression, the superposition of two monolayers may occur together with a slight rearrangement of their in-plane structure. Moreover, the triflate counterions attached to the grid units were assumed to occupy the same positions as found in the initial monolayer structure, which is not necessarily correct. Furthermore, the possibility of a film composed of more than two layers cannot be discarded.

We conclude that, irrespective of the precise structure, during the film compression the initially self-assembled monolayer undergoes a transition to a crystalline bi(multi)-layer of almost unchanged in-plane arrangement. This system is, to our knowledge, the first example of a complex architecture that self-assembles into a crystalline monolayer

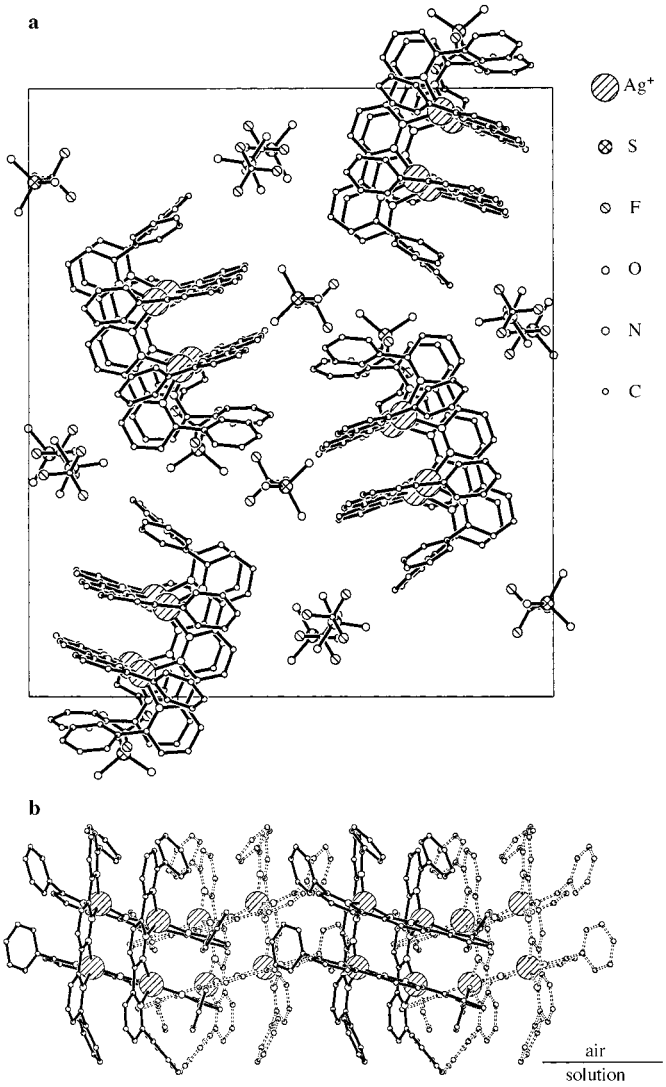

Figure 9. Packing arrangement of the 2×2 Ag^+ grid complex in the self-assembled monolayer domains viewed: a) perpendicular and b) parallel to the solution surface. Ag^+ ions are shown as hatched large circles. Note that in b) the dashed lines belong to molecules that are behind those in solid lines.

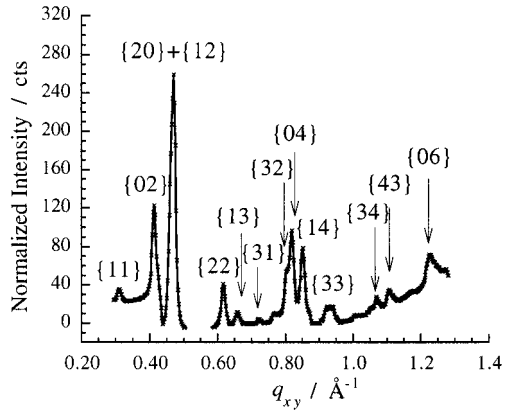

Figure 10. Measured GIXD data of ligand **1**, spread on 1 mM CF_3SO_3Ag aqueous solution after compression to a nominal mean molecular area of 10 Å^2, presented as intensity distribution $I(q_{xy})$ and showing the Bragg peaks with assigned (h,k) Miller indices.

Table 5. Analysis of the GIXD data measured from the crystalline bilayer of the 2×2 Ag^+ grid complex, $[Ag_4\mathbf{1}_4][(CF_3SO_3)_4]$ obtained by compression of the initial monolayer at the air–solution interface. The calculated q_{xy} values are from the unit cell of dimensions $a = 26.86$ Å, $b = 30.43$ Å, $A_{cell} = 817$ Å^2.

Peak no.	q_{xy} [Å^{-1}] measured	{h,k} Miller index assigned	q_{xy} [Å^{-1}] calculated
1	0.312	{11}	0.312
2	0.413	{02}	0.413
3	0.464	{20}	0.468
4	0.473	{12}	0.475
5	0.618	{22}	0.624
6	0.658	{13}	0.662
7	0.720	{31}	0.731
8	0.765	{23}	0.776
9	0.805	{32}	0.814
10	0.820	{04}	0.826
11	0.860	{14}	0.858
12	0.940	{33}	0.936
13	1.07	{34}	1.083
14	1.11	{43}	1.122
15	1.23	{06}	1.239

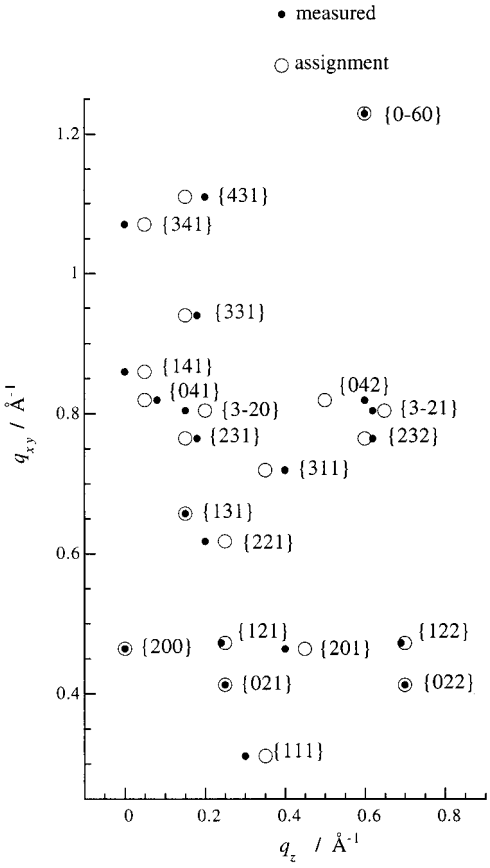

Figure 11. Two-dimensional q_{xy},q_z plot showing measured (filled circles) and calculated (empty circles) positions of the Bragg rod intensity $I(q_z)$ modulations assigned with l Miller indices for the 15 (h,k,q_z) Bragg reflections of the crystalline bilayer.

and then undergoes a phase transition to a crystalline bilayer. Note that the transition from a crystalline monolayer to a crystalline bilayer could be prevented when the 2×2 Ag^+ grid complex was self-assembled in the presence of a 1:1 acetate/triflate counterions. For this system, the GIXD patterns (not shown), measured before and after compression, are consis-

0947-6539/00/0604-0732 $ 17.50+.50/0 *Chem. Eur. J.* **2000**, *6*, No. 4

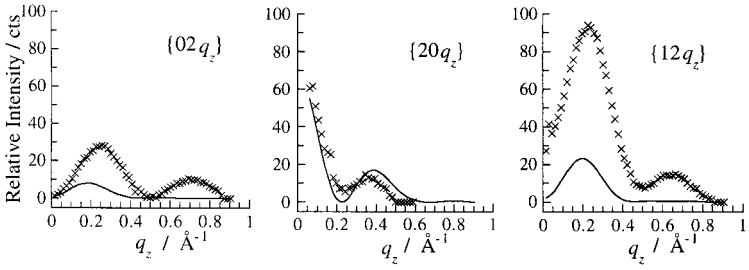

Figure 12. Measured (points) and calculated (solid line) Bragg rod intensity profiles $I(q_z)$ for the $(02q_z)$, $(20q_z)$, and $(12q_z)$ reflections of the crystalline bilayer.

tent with the self-assembled crystalline monolayer of the same structure as that formed with triflate counterions. On silver acetate solution, no GIXD pattern was observed; this is indicative of an interfacial reaction (due to disappearance of the free ligand GIXD pattern) but a soluble product formation, in agreement with the Π-A isotherm. The formation of a crystalline bilayer over silver triflate solution, of a monolayer over mixed silver acetate/triflate solution, and the absence of a film on silver acetate subphase from the same amount of free ligand molecule can be explained in terms of the different solubilities of the complex salt with various counterions; this is in keeping with the Π-A isotherms of the three systems (Figure 1).

Conclusion

This study describes a two-step process of an interfacial reaction between free ligand molecules and the Ag^+ ions contained in the subphase (with triflate and mixed acetate/triflate counterions) leading to the formation of a 2×2 Ag^+ grid complex followed by its self-assembly into an oriented crystalline monolayer. The two-dimensional crystal structure analysis made use of the SHELX-97 computer program. On surface compression, the initial self-assembled monolayer formed on silver triflate solution undergoes a transition to a crystalline bilayer, almost retaining the initial in-plane arrangement. The ability to design thin oriented films of 2×2 Ag^+ grid complexes, composed of defined number of metal ions in a confined geometry, may lead to organometallic composites that contain homodisperse semiconducting or conducting particles with new optoelectronic properties.

Experimental Section

The syntheses of the ligand 3,6-bis[2-(6-phenylpyridine)]pyridazine **1**, and the 2×2 Ag^+ grid complex $[Ag_4\mathbf{1}_4][(CF_3SO_3)_4]$ prepared in bulk solution have been described elsewhere.[12] The thin films of the $2 \times 2Ag^+$ grid complex were prepared by spreading free ligand molecules **1**, from 0.5 mM solutions in chloroform, onto a 1 mM aqueous solution of silver triflate (CF_3SO_3Ag purchased from Sigma). The surface pressure area (Π-A) isotherms were performed on an automatic Lauda trough (in the dark when silver triflate aqueous solutions were used).

XPS and SFM measurements: Measurements were performed on samples prepared in a specially constructed teflon trough (surface area 20 cm^2) in which the solid supports were inserted into the subphase prior to spreading the chloroform solution of the free ligand molecules. The solid supports used were glass slides (1×1 cm) for XPS and freshly cleaved mica pieces (1×1 cm) for SFM. After spreading the solution of **1** for a nominal molecular area of 30 Å^2, a reaction time of 30 minutes was allowed prior to cooling the subphase from 20 °C to 5 °C. After an additional 30 minutes, the liquid subphase was slowly drained with a motor-driven syringe.

SFM measurements: These were performed on a Topometrix TMX2010 Discoverer system in intermittent contact mode with integrated Si tip/cantilevers and a resonance frequency of 260–330 kHz (Nanoprobe), or in contact mode with integrated Si_3N_4 tip/cantilever and an SPJ constant ~ 0.2 N m^{-1} (Park Scientific).

XPS measurements: These were performed on a commercial AXIS-HS Kratos set-up, with a monochromatized Al(Kα) source (5 mA emission current at 15 KV) and pass energies of 20–80 eV. A flood gun was used for the neutralization of the surface, and the final energy scaling was determined by the glass support Si(2p) line (103.3 eV). Possible potential gradients across the film were estimated to be 0.1 eV at most. Spectra of reference bulk samples, for which the Si(2p) line could not be used, were scaled with respect to the Ag(3d) line. Data analysis included decomposition of the photoelectron lines into Gaussian–Lorenzian components superimposed on a Shirley background.[22] We checked the role of beam-induced damage by comparing the spectra measured at various exposure times and used this information to get exposure times that minimize the damage. In order to maintain exposure periods below 3 minutes for the low intensity signals [e.g., the N(1s) and C(1s) lines] it was necessary to shift the sample between sequential scans to fresh areas. The homogeneity of the samples on the mm to cm scale was verified to be very good, allowing this procedure for minimizing the beam-induced damage.

Grazing-incidence X-ray diffraction (GIXD): The experiments were performed on the liquid-surface diffractometer at the undulator synchrotron beam line BW1 in HASYLAB at DESY (Hamburg). When silver triflate solutions were used as subphase, the film preparation was done in red light. Measurements were performed, at different points along the 5 °C isotherms. A detailed description of the GIXD method is given elsewhere.[5, 23] The incidence angle, α_i of the monochromated X-ray beam was adjusted to be approximately equal to $0.85\alpha_c$ ($\alpha_c \approx 0.138°$ is the critical angle for total external reflection of the X-rays from a water surface), which maximizes the surface sensitivity relative to bulk. The dimensions of the fingerprint of the incoming X-ray beam on the liquid surface were $\sim 5 \times 50$ mm^2 (or $\sim 2 \times 50$ mm^2). GIXD diffraction peaks were obtained from two-dimensional crystallites with an azimuthally random orientation. The scattered intensity was detected by a position-sensitive detector (PSD) along the vertical component of the X-ray scattering vector, $q_z \approx (2\pi/\lambda)\sin\alpha_f$, in which α_f is the angle between the horizon and the diffracted beam. Measurements were performed by scanning over a range along the horizontal scattering vector, $q_{xy} \approx (4\pi/\lambda)\sin\theta_{xy}$, in which $2\theta_{xy}$ is the angle between the incident and diffracted beams projected onto the horizontal plane. Note that the scattering vector $\boldsymbol{q}$ is equal to $\boldsymbol{q_{xy}} + \boldsymbol{q_z}$. The diffraction data are represented in three ways: i) primarily, as a two-dimensional intensity distribution $I(q_{xy},q_z)$; ii) the GIXD pattern $I(q_{xy})$, obtained by integration over the whole q_z window of the PSD, that shows Bragg peaks; iii) Bragg rod intensity profiles, which are the scattered intensity $I(q_z)$ recorded in channels along the PSD but integrated (after background subtraction) across the q_{xy} range of each Bragg peak. Several different types of information were extracted from the measured profiles.[5] The $2\theta_{xy}$ (or q_{xy}) positions of the Bragg peaks yield the lattice repeat distances $d = 2\pi/q_{xy}$, which can be indexed by two Miller indices (h and k) to yield the unit cell. The full width at half maximum of the Bragg peaks along q_{xy} [FWHM(q_{xy})] yields an estimate of the two-dimensional crystalline coherence length, $L \approx 0.88 \times 2\pi/\mathrm{FWHM}(q_{xy})$.[24] The FWHM of the Bragg rod intensity profile along q_z [FWHM(q_z)] gives an estimate of the crystallite thickness $\approx 0.88 \times 2\pi/\mathrm{FWHM}(q_z)$. The separation along q_z between various intensity modulations gives a first estimate of the lattice spacing in the direction perpendicular to the liquid surface $\approx 2\pi/\Delta q_z$. The intensity at a particular value in a Bragg rod is determined by the square of the molecular structure factor $|F_{hk}(q_z)|^2$, thus allowing its evaluation

according to an atomic coordinate model of the molecules. The CERIUS[2] molecular simulation package[25] and SHELX-97[20] computer programs were used for structure determination.

Specular X-ray reflectivity (XR): Measurements, with the same liquid surface diffractometer as for the GIXD, were performed by scanning the incident beam (α_i), equal to the reflected (α_f) beam angles, from $0.5\alpha_c$ to $40\alpha_c$. The detection of the reflected radiation was measured by an NaI scintillation counter. The experimental results are given in the form of normalized X-ray reflectivity R/R_F, in which R_F is the "Fresnel" reflectivity calculated for a perfect sharp interface as a function of the normalized vertical scattering vector q_z/q_c, in which $q_z = (4\pi/\lambda)\sin\alpha_i$ and $q_c = (4\pi/\lambda)\sin\alpha_c$ is the scattering vector at the critical angle of incidence.

Acknowledgements

We acknowledge the financial support provided by the AFIRST (Association Franco-Israelienne pour la Recherche Scientifique et Technologique) grant no. 9814-1-98, the Petroleum Research Fund of the American Chemical Society, the Danish Foundation for Natural Sciences, and the TMR-Contract ERBFMGECT950059 of the European Community. We are grateful to HASYLAB at DESY, Hamburg, for beam time at BW1 line and for support.

[1] F. Leveiller, D. Jacquemain, M. Lahav, L. Leiserowitz, M. Deutsch, K. Kjaer, J. Als-Nielsen, *Science* **1991**, *252*, 1532.
[2] I. Kuzmenko, R. Buller, W. Bouwman, K. Kjaer, J. Als-Nielsen, M.Lahav, L. Leiserowitz, *Science* **1996**, *274*, 1046.
[3] I. Weissbuch, J. Majewski, K. Kjaer, J. Als-Nielsen, M. Lahav, L. Leiserowitz, *J. Phys.Chem.* **1993**, *97*, 12848.
[4] I. Weissbuch, S. Guo, S. Cohen, R. Edgar, P. Howes, K. Kjaer, J. Als-Nielsen, M. Lahav, L. Leiserowitz, *Adv. Mat.* **1998**, *10*, 117.
[5] I. Weissbuch, R. Popovitz-Biro, M. Lahav, L. Leiserowitz, K. Kjaer, J. Als-Nielsen, in *Advances in Chemical Physics*, *Vol. 102* (Eds.: S. Rice, I. Prigogine), Wiley, **1997**, pp. 39–121.
[6] F. Leveiller, C. Böhm, D. Jacquemain, H. Möhwald, L. Leiserowitz, K. Kjaer, J. Als-Nielsen, *Langmuir* **1994**, *10*, 819.
[7] C. Böhm, F. Leveiller, D. Jacquemain, H. Möhwald, K. Kjaer, J. Als-Nielsen, I. Weissbuch, L. Leiserowitz, *Langmuir* **1994**, *10*, 830.
[8] J.-M. Lehn, *Supramolecular Chemistry Concepts and Perspectives*, *Vol. 9*, VCH, Weinheim (Germany), **1995**.
[9] P. Baxter, J.-M. Lehn, A. DeCian, J. Fischer, *Angew. Chem.* **1993**, *105*, 92; *Angew. Chem. Int. Ed. Engl.* **1993**, *32*, 69.
[10] P. N. W. Baxter, J.-M. Lehn, J. Fischer, M.-T. Youinou, *Angew. Chem.* **1994**, *106*, 2432; *Angew. Chem. Int. Ed. Engl.* **1994**, *33*, 2284.
[11] P. N. W. Baxter, G. S. Hanan, J.-M. Lehn, *Chem. Commun.* **1996**, 2019.
[12] P. N. W. Baxter, J.-M. Lehn, B. O. Kneisel, D. Fenske, *Angew. Chem.* **1997**, *109*, 2067; *Angew. Chem. Int. Ed. Engl.* **1997**, *36*, 1978.
[13] G. S. Hanan, D. Volkner, U. S. Schubert, J.-M. Lehn, G. Baum, D. Fenske, *Angew. Chem.* **1997**, *109*, 1929; *Angew. Chem. Int. Ed. Engl.* **1997**, *36*, 1842.
[14] I. Weissbuch, P. Baxter, S. Cohen, H. Cohen, K. Kjaer, P. B. Howes, J. Als-Nielsen, G. S. Hanan, U. S. Schubert, J.-M. Lehn, L. Leiserowitz, M. Lahav, *J. Am. Chem. Soc.* **1998**, *120*, 4850.
[15] The C(1s) line measured for the grid bulk was fitted with the same four components to which a fifth component was added in order to consider the contribution of the tape used to glue the powder on the holder (not shown).
[16] Note that the observed reflectivity curve did not change after compression of the film which induced a transition to the crystalline bilayer, as determined from the GIXD measurements on the same sample, and repeated several times.
[17] In terms of the molecular dimensions of **1**, the unit cell may contain two molecules oriented with the molecular plane parallel to the air–water interface (see ref. [14]). The *d* spacing of 5.5 Å may correspond to the stacking of the molecules.
[18] As reported for other systems spread on Ag^+ containing solutions (see ref. [14]), the GIXD pattern shows three additional peaks at q_{xy} values of 1.95, 2.26, and 3.20 $Å^{-1}$. In contrast with all the other peaks, these three peaks are highly skewed along $q_t = (q_{xy}^2 + q_z^2)^{1/2} = \text{constant}$; this denotes random orientation with respect to the surface. We assign these peaks as belonging to microcrystals of AgCl, since, in accordance to the Inorganic Powder Diffraction File, they correspond to the (111), (200), and (220) reflections of AgCl with *d* spacings of 3.20 Å, 2.77 Å, and 1.96 Å, respectively. We account for the presence of these three peaks in various systems by formation of AgCl due to the presence of traces of Cl^- ions in the ligand compound.
[19] The atomic coordinates of the crystal structure reported by M.-T. Youinou, N. Rahmouni, J. Fischer, J. A. Osborn, *Angew. Chem.* **1992**, *104*, 771; *Angew. Chem. Int. Ed. Engl.* **1992**, *31*, 733, were used as a basis for the model.
[20] G. M. Sheldrick, SHELX-97 Program for Crystal Structure Determination, University of Göttingen, **1997**.
[21] The measured $\{20q_z\} + \{12q_z\}$ Bragg rod intensities are superimposed (Figure 7a). For the refinement with SHELX-97 they were separated into two individual rods on the basis of their $I(h,k)$ intensity ratio calculated with Cerius[2].
[22] A. D. Shirley, *Phys. Rev. B* **1972**, *5*, 4709.
[23] J. Als-Nielsen, D. Jacquemain, K. Kjaer, F. Leveiller, M. Lahav, L. Leiserowitz, *Phys. Rep.* **1994**, *246*, 251.
[24] A. Guinier, *X-Ray Diffraction*, Freeman, San Francisco, **1963**.
[25] CERIUS[2], molecular modeling software for materials research from BIOSYM/Molecular Simulations, San Diego CA (USA) and Cambridge (UK).

Received: May 11, 1999 [F1780]

  0947-6539/00/0604-0734 $ 17.50+.50/0